ЖУРНАЛ ФІЗИЧНИХ ДОСЛІДЖЕНЬ
т. 14, № 3 (2010) 3701(11 с.)

JOURNAL OF PHYSICAL STUDIES
v. 14, No. 3 (2010) 3701(11 p.)

THE THERMODYNAMICS OF THE ROCHELLE SALT $NaKC_4H_4O_6{\cdot}4H_2O$ CRYSTAL STUDIED WITHIN THE MITSUI MODEL EXTENDED BY PIEZOELECTRIC INTERACTION AND TRANSVERSE FIELD

R. R. Levitskii[1], I. R. Zachek[2], A. Ya. Andrusyk[1]
[1] *Institute for Condensed Matter Physics of the National Academy of Sciences of Ukraine, 1 Sventsitsky St., 79011 Lviv, Ukraine*
[2] *Lviv Polytechnic National University, 12 Bandera St., 79013 Lviv, Ukraine*
(Received December 28, 2009)

We calculated dielectric, piezoelectric and elastic properties of the Rochelle salt within the Mitsui model extended by piezoelectric interaction and transverse field. This field occurs due to dynamic flipping of ordering structure elements between two equilibrium positions. We the studied static characteristics within molecular field approximation. We derived unique parameter set that allows us to achieve a better description of the physical characteristics (particularly for spontaneous polarization) as compared with the analogous model that does not take into account transverse field.
Key words: Rochelle salt, dielectric response, molecular field approximation.

PACS number(s): 77.22.Ch, 77.22.Gm, 77.65.Bn, 77.80.Bh

I. INTRODUCTION

Ferroelectric crystals of the order–disorder type with asymmetric double-well potential has a number of unusual properties. A good example of such crystal is sodium potassium tartrate tetrahydrate $NaKC_4H_4O_6{\cdot}4H_2O$ (Rochelle salt or Rs). It is generally accepted that this crystal has two Curie points, $T_{c1} = 255$ K and $T_{c2} = 297$ K, being ferroelectric in a rather narrow temperature range between T_{c1} and T_{c2} [1]. Both phase transitions are of the second order.

Structural studies hold a prominent place in the study of the Rochelle salt. The crystalline structure of Rs proved to be complex. It is orthorhombic (space group $D_2^3 - P2_12_12_1$) in the paraelectric phases and monoclinic (space group $C_2^2 - P2_1$) in the ferroelectric phase [2]. Spontaneous polarization is directed along the a crystal axis; it is accompanied by a spontaneous shear strain ε_4. There are four formula units (112 atoms) in the unit cell of the Rochelle salt. The unit cell is divided into four nonequivalent structural elements each of which produces a dipole moment both along ferroelectric x- and along y-axes. Consequently, a crystal lattice is divided into for sublattices. Recent studies [3] based on X-ray diffraction data, argued that it is the order–disorder motions of O9 and O10 groups, coupled with the displacive vibrations of O8 groups, which were responsible for the phase transitions in the Rochelle salt as well as for the spontaneous polarization.

Inspite of the achievements in the determination of Rochelle salt structure, hydrogen atoms arrangement in the crystal and their role in phase transition still remains unclear. Their important role is testified by significant hydrogen/deuterium isotope effect. Such situation makes *ab initio* calculations impossible and requires the application of alternative approaches.

We study Rochelle salt properties within the semimicroscopic approach, which is based on the assumption that phase transition in Rochelle salt is of order–disorder type. This assumption is supported by system dielectric response of relaxation type, which was derived for microwave region [4–6]. Besides that, neutron diffraction experimental data [7] supported the presence of two possible ionic configurations. The dielectric [8], spectroscopic (Raman spectrum) [9] and structural (neutron scattering) [10] studies, carried out in submillimeter range, indicate the presence of system resonance response, which is over-damped once it approaches the point of phase transition from the low-temperature paraelectric phase, and it is evidence of phase transition of the displacement type.

On the other hand, this resonance response may be caused by a dynamic flipping of structural elements between two equilibrium positions. One may expect that the introduction of additional term like transverse field, responsible for dynamic flipping of structural elements, into a model Hamiltonian will permit the description of this resonance response. Thus, a simple model like de Gennes one can be applicable to the description of Rochelle salt properties.

Mitsui proposed a model of the order–disorder type adequate to Rochelle salt [11]. This model is based on the assumption that structural elements move between two equilibrium positions. Each cell contains two dipoles; the potential barrier between two equilibrium orientations of a dipole is asymmetric. The dipoles form two competitive sublattices with local potentials, which are the mirror reflections of each other. Therefore, even though dipoles in each sublattice are always ordered (sublattice polarization is available), the total polarization at certain temperatures can equal zero.

The study of the Mitsui model, formulated in terms of pseudospin operators [5, 12], reveals several types of temperature behavior of the model. Depending on the values of model parameters, it can undergo, for instance, a single second order phase transition from ferroelectric

into paraelectric phase (observed in $RbHSO_4$), two second order phase transitions (Rs, dRs), one low temperature first order and one high temperature second order phase transition[1] (NH_4HSO_4), etc. The spontaneous polarization, dielectric permittivity and other thermodynamic characteristics of the crystals mentioned above were calculated and studied within the Mitsui model in the molecular field approximation [12–15].

The relaxation dynamics of the Rs, dRs and $RbHSO_4$ was explored within the Mitsui model too [12, 15–19], where the temperature dependence of relaxation times and dynamic permittivity of these crystals were calculated. Concerning Rochelle salt, it was obtained that relaxation time, exhibiting a critical slowing down at the Curie points, actually diverges at these points. However, experiments [5] indicate that the value of relaxation time is large but remains finite. Also, theoretically calculated and experimental static dielectric permittivities are essentially different: the former diverges at the phase transition points whereas the last remains finite. Naturally, such inconsistency appears either due to the model incompletion or due to approximation. Latter the Mitsui model was extended by means of accounting tunnelling effects [12,16]. However, this improvements failed to provide for the correct temperature dependence of relaxation time at the phase transition points.

The problem of incorrect temperature dependence of relaxation times and dynamic permittivity for Rs crystal at the Curie points was successfully solved by taking into account piezoelectric interaction of pseudospin subsystem with lattice deformation [20]. Finite relaxation time at the phase transition points was obtained within the extended Mitsui model. This approach allows to explain the experimentally detected difference of static permittivities of clamped and free crystals. Generally, a good agreement of theory and experiment for dielectric permittivities of clamped and free crystals was derived [20]. The unique theory parameter set, providing acceptable agreement of theory and experiment for numerous physical characteristics of the Rochelle salt: elastic, longitudinal dielectric (static and dynamic) and piezoelectric, was derived for the first time in this work.

Recent works deal with new theoretical consideration of the influence produced by external factors like field [21], hydrostatic [22] and uniaxial σ_4 [23] pressures on the physical properties of Rs. The influence of a partial deuteration on Rochelle salt was studied within extended Mitsui model [24] as well as piezoelectric resonance in Rs [25]. Also, experiments [26] for the effect of humidity, annealing, stresses, electric field on dielectric permittivity of Rochelle salt were carried out. Modern experimental techniques, applied therein, updated experimental data, formerly derived for Rs crystal.

Notwithstanding the significant advances in studying Rs crystal, some problems concerning the theoretical explanation of Rochelle salt physical properties still remain unresolved. Thus, the theoretically calculated value of spontaneous polarization appeared to be significantly lower than the experimental one along the whole temperature range.

We can identify several ways of dealing with the existing problems. For instance, the model can be supplemented with accounting for electrostriction forces, transverse field (arising due to the flipping of ordering units between two equilibrium position); it can be extended from order–disorder type to mixed type — displacive and order–disorder (distinctly accounting for a couple of pseudospin modes with lattice modes of displacement). Therewith, taking into consideration the real structure of Rochelle salt crystal it is worth analyzing the four-sublattice Mitsui model [27] (having previously supplemented it with accounting for the piezoelectric interaction) instead of the two-sublattice Mitsui model. To deal with the problems existing in theory of physical properties of Rochelle salt, it is also appropriate to use higher approximations (e.g., a two-particle cluster approximation) while analyzing Mitsui type Hamiltonians extended by piezoelectric interaction. In this paper we supplemented the extended Mitsui model [20] by accounting for transverse field.

In order to select the theory parameters the general problem of possible phase transitions in the Mitsui model should be solved. Vaks [13] made the first attempt to study possible phase transitions in the Mitsui model. However, the obtained diagram is quite approximate and leaves transverse field out of consideration. Recently the correct phase diagram of the Mitsui model in a molecular field approximation was constructed [28,29]. It enabled a comprehensive analysis of Rochelle salt within the Mitsui model. More specifically, it became possible to select the optimum set of theory parameters for describing several physical properties of Rochelle salt simultaneously.

In the present work using the phase diagram of the Mitsui model we obtained a set of theory model parameters and on the base thereof we calculated dielectric (static and dynamic), piezoelectric, elastic and heat properties of Rochelle salt. Within the framework of this research we attempted to find out whether consideration of transverse field can explain the experimental temperature dependence of the spontaneous polarization.

The Mitsui model, extended with transverse field, has been already used for analysis of physical properties of Rochelle salt [13–16] (earlier works erroneously attributed transverse field to tunnelling of the protons, considered them to be ordering units), however, those works did not take into consideration piezoelectric interaction, which is significant for the theoretical description of Rochelle salt, and furthermore, they were restricted to the description of only one or two physical properties.

[1]Here the additional assumption that the model parameters slightly depend on temperature is needed.

II. THERMODYNAMIC CHARACTERISTICS OF THE EXTENDED MITSUI MODEL

We give consideration to a two-sublattice piezoelectric order–disorder type system with an asymmetric double-well potential. The Hamiltonian of such a system is referred to as the Mitsui Hamiltonian. We assume this system has essential piezoelectric interaction which should be accounted for. Besides, the model requires that the transverse field is accounted. We suppose the polarization is directed along x-axes and arises due to the structural units ordering in the one of two possible equilibrium positions. We consider the situation when ε_4 component of strain tensor effects the energy of these equilibrium positions. Precisely this case occurs in Rs. We complement the modified Mitsui Hamiltonian [20], with transverse field to take into account the possibility of dynamic ordering units flipping between two equilibrium positions. The resulting Hamiltonian is of the following form:

$$\begin{aligned} H = &\sum_q \left[\frac{1}{2} v c_{44}^{E0} \varepsilon_4^2 - v e_{14}^0 E_{1q} \varepsilon_4 - \frac{1}{2} v \chi_{11}^{\varepsilon 0} E_{1q}^2\right] \\ &- \sum_{q,q'} \left[\frac{J_{qq'}}{2} (S_{q1}^z S_{q'1}^z + S_{q2}^z S_{q'2}^z) + K_{qq'} S_{q1}^z S_{q'2}^z\right] \\ &- \sum_{qf} \left[\Omega S_{qf}^x + (\Delta_f - 2\psi_4 \varepsilon_4 + \mu E_{1q}) S_{qf}^z\right]. \end{aligned} \tag{1}$$

Three terms in the first sum of Eq. (1) represent the elastic, piezoelectric, and electric energies attributed to a host lattice, in which potential the pseudospin moves (with the "seed" elastic constant c_{44}^{E0}, the coefficient of piezoelectric stress e_{14}^0, and dielectric susceptibility $\chi_{11}^{\varepsilon 0}$); v is a volume of cell containing a pair of pseudospins (ordering units or dipoles) of one lattice site $\mathbf{q}$ and different sublattices $f = 1, 2$ (further we will call it a unit cell[2]). The second sum describes direct interaction of the ordering units: $J_{qq'} = J_{q'q}$ and $K_{qq'} = K_{q'q}$ are interaction potentials between pseudospins belonging to the same and to different sublattices, respectively. The first term in the third sum is the transverse field; the second term describes: (a) energy, associated with asymmetry of the potential, where Δ_f is asymmetry parameter: $\Delta_1 = -\Delta_2 = \Delta$; (b) interaction energy of pseudospin with the field arising due to the piezoelectric deformation and ψ_4 is a parameter of piezoelectric interaction; (c) interaction energy of pseudospin with external electric field E_{1q}, where μ is an effective dipole moment of the model unit cell.

We carry out the study within the mean field approximation (MFA). Performing identical transformation

$$S_{qf}^z = \left\langle S_{qf}^z \right\rangle + \Delta S_{qf}^z \tag{2}$$

and neglecting the quadratic fluctuations we rewrite the initial Hamiltonian (1) as

$$\begin{aligned} H_{\mathrm{MFA}} = &\sum_q \left[\frac{1}{2} v c_{44}^{E0} \varepsilon_4^2 - v e_{14}^0 E_{1q} \varepsilon_4 - \frac{1}{2} v \chi_{11}^{\varepsilon 0} E_{1q}^2\right] \\ &+ \sum_{qq'} \left[\frac{1}{2} J_{qq'} \left(\left\langle S_{q1}^z \right\rangle \left\langle S_{q'1}^z \right\rangle + \left\langle S_{q2}^z \right\rangle \left\langle S_{q'2}^z \right\rangle\right) \right. \\ &\left. + K_{qq'} \left\langle S_{q1}^z \right\rangle \left\langle S_{q'2}^z \right\rangle\right] - \sum_{qf} \boldsymbol{\mathcal{H}}_{qf} \boldsymbol{S}_{qf}, \end{aligned} \tag{3}$$

where $\boldsymbol{\mathcal{H}}_{qf}$ are the mean local fields having effect on the pseudospins $\boldsymbol{S}_{qf}$:

$$\mathcal{H}_{qf}^x = \Omega, \quad \mathcal{H}_{qf}^y = 0, \quad \mathcal{H}_{qf}^z = \varepsilon_{qf},$$

$$\begin{aligned} \varepsilon_{q1} = &\sum_{q'} \left[J_{qq'} \left\langle S_{q'1}^z \right\rangle + K_{qq'} \left\langle S_{q'2}^z \right\rangle\right] \\ &+ \Delta - 2\psi_4 \varepsilon_4 + \mu E_{1q}, \end{aligned} \tag{4a}$$

$$\begin{aligned} \varepsilon_{q2} = &\sum_{q'} \left[J_{qq'} \left\langle S_{q'2}^z \right\rangle + K_{qq'} \left\langle S_{q'1}^z \right\rangle\right] \\ &- \Delta - 2\psi_4 \varepsilon_4 + \mu E_{1q}. \end{aligned} \tag{4b}$$

Within MFA we can calculate mean equilibrium values of the pseudospin operators:

$$\langle \boldsymbol{S}_{qf} \rangle = \mathrm{Sp}(\boldsymbol{S}_{qf} \rho_{\mathrm{MFA}}), \tag{5}$$

where

$$\rho_{\mathrm{MFA}} = \frac{\exp\left(-\frac{H_{\mathrm{MFA}}}{k_{\mathrm{B}} T}\right)}{\mathrm{Sp} \exp\left(-\frac{H_{\mathrm{MFA}}}{k_{\mathrm{B}} T}\right)}. \tag{6}$$

After calculations we derive

$$\langle \boldsymbol{S}_{qf} \rangle = \frac{1}{2} \frac{\boldsymbol{\mathcal{H}}_{qf}}{\mathcal{H}_{qf}} \tanh \frac{\mathcal{H}_{qf}}{2 k_{\mathrm{B}} T}, \tag{7}$$

where $\mathcal{H}_{qf} \equiv |\boldsymbol{\mathcal{H}}_{qf}| = \lambda_{qf}$.

The crystals' free energy within MFA

$$F(4) = -k_{\mathrm{B}} T \ln \mathrm{Sp} \exp\left(-\frac{H_{\mathrm{MFA}}}{k_{\mathrm{B}} T}\right)$$

is a follows:

$$\begin{aligned} F(4) = &\sum_q \left[\frac{1}{2} v c_{44}^{E0} \varepsilon_4^2 - v e_{14}^0 E_{1q} \varepsilon_4 - \frac{1}{2} v \chi_{11}^{\varepsilon 0} E_{1q}^2\right] \\ &+ \sum_{qq'} \left[\frac{1}{2} J_{qq'} \left(\left\langle S_{q1}^z \right\rangle \left\langle S_{q'1}^z \right\rangle + \left\langle S_{q2}^z \right\rangle \left\langle S_{q'2}^z \right\rangle\right) \right. \\ &\left. + K_{qq'} \left\langle S_{q1}^z \right\rangle \left\langle S_{q'2}^z \right\rangle\right] \\ &- k_{\mathrm{B}} T \sum_{qf} \ln\left(2 \cosh \frac{\lambda_{qf}}{2 k_{\mathrm{B}} T}\right). \end{aligned} \tag{8}$$

[2]The actual unit cell of the Rochelle salt crystal contains two pairs of pseudospins of two lattice sites and different sublattices; therefore, we should set the value of the model unit cell volume to be half of the crystal unit cell volume.

In the homogeneous external field the set of $6N$ equations (7) (where N is the number of lattice sites) has a lot of solutions with a homogeneous one among others: $\langle \boldsymbol{S}_{qf}\rangle \equiv \langle \boldsymbol{S}_{qf}\rangle_0 \neq f(q)$. In Rochelle salt crystal case we have $J_{qq'}, K_{qq'} > 0$ and it is a homogeneous solution which provides the free energy minimum. In this case, a set of equations reduces into the system

$$\langle \boldsymbol{S}_{qf}\rangle_0 = \frac{1}{2}\frac{\boldsymbol{\mathcal{H}}_f^{(0)}}{\mathcal{H}_f^{(0)}}\,\tanh\frac{\mathcal{H}_f^{(0)}}{2k_{\mathrm{B}}T}, \tag{9}$$

where the local field $\boldsymbol{\mathcal{H}}_f^{(0)}$ is the following:

$$\mathcal{H}_f^{(0)x} = \Omega, \qquad \mathcal{H}_f^{(0)y} = 0, \qquad \mathcal{H}_f^{(0)z} = \varepsilon_f, \tag{10}$$

$$\varepsilon_1 = J_0\left\langle S_{q1}^z\right\rangle_0 + K_0\left\langle S_{q2}^z\right\rangle_0 + \Delta - 2\psi_4\varepsilon_4 + \mu E_1, \tag{11a}$$

$$\varepsilon_2 = J_0\left\langle S_{q2}^z\right\rangle_0 + K_0\left\langle S_{q1}^z\right\rangle_0 - \Delta - 2\psi_4\varepsilon_4 + \mu E_1, \tag{11b}$$

where

$$J_0 = \sum_{q'} J_{qq'}, \qquad K_0 = \sum_{q'} K_{qq'};$$
$$\mathcal{H}_f^{(0)} \equiv \left|\boldsymbol{\mathcal{H}}_f^{(0)}\right| = \lambda_f, \qquad \lambda_f = \sqrt{\Omega^2 + \varepsilon_f^2}.$$

The z-component of this equation system forms the two-equation system ($f = 1, 2$) to determine $\left\langle S_{qf}^z\right\rangle_0$:

$$\left\langle S_{qf}^z\right\rangle_0 = \frac{\varepsilon_f}{2\lambda_f}\,\tanh\frac{\lambda_f}{2k_{\mathrm{B}}T}. \tag{12}$$

Having introduced new variables

$$\boldsymbol{\xi} = \langle \boldsymbol{S}_{q1}\rangle_0 + \langle \boldsymbol{S}_{q2}\rangle_0, \qquad \boldsymbol{\sigma} = \langle \boldsymbol{S}_{q1}\rangle_0 - \langle \boldsymbol{S}_{q2}\rangle_0 \tag{13}$$

(ξ^z and σ^z are ferroelectric and antiferroelectric ordering parameters), we obtain a system of equations (12) in the form:

$$\begin{cases} \xi^z &= \dfrac{1}{2}\Big[\dfrac{\tilde\varepsilon_1}{\tilde\lambda_1}\,\tanh\dfrac{\tilde\lambda_1}{2T} + \dfrac{\tilde\varepsilon_2}{\tilde\lambda_2}\,\tanh\dfrac{\tilde\lambda_2}{2T}\Big], \\ \sigma^z &= \dfrac{1}{2}\Big[\dfrac{\tilde\varepsilon_1}{\tilde\lambda_1}\,\tanh\dfrac{\tilde\lambda_1}{2T} - \dfrac{\tilde\varepsilon_2}{\tilde\lambda_2}\,\tanh\dfrac{\tilde\lambda_2}{2T}\Big], \end{cases} \tag{14}$$

where the unknown ξ^z and σ^z are defined at a given T, E_1, ε_4. In system (14) the following notations are used:

$$\tilde\varepsilon_f = \varepsilon_f/k_{\mathrm{B}}, \quad \tilde\lambda_f = \sqrt{\tilde\Omega^2 + \tilde\varepsilon_f^2},$$
$$\tilde\varepsilon_1 = \tilde R_0^+\xi^z + \tilde R_0^-\sigma^z + \tilde\Delta - 2\tilde\psi_4\varepsilon_4 + \tilde\mu E_1, \tag{15}$$
$$\tilde\varepsilon_2 = \tilde R_0^+\xi^z - \tilde R_0^-\sigma^z - \tilde\Delta - 2\tilde\psi_4\varepsilon_4 + \tilde\mu E_1.$$

Here

$$\tilde\Omega = \Omega/k_{\mathrm{B}}, \ \ \tilde\Delta = \Delta/k_{\mathrm{B}}, \ \ \tilde\psi_4 = \psi_4/k_{\mathrm{B}}, \ \ \tilde\mu = \mu/k_{\mathrm{B}},$$
$$\tilde R_0^{\pm} = \frac{\tilde J_0 \pm \tilde K_0}{2}, \quad \tilde J_0 = \frac{J_0}{k_{\mathrm{B}}}, \quad \tilde K_0 = \frac{K_0}{k_{\mathrm{B}}}. \tag{16}$$

System (14) is a system of two equations with the variables ξ^z and σ^z.

When the values ξ^z and σ^z are defined we can calculate the values ξ^x and σ^x using (9) and (13):

$$\xi^x = \frac{1}{2}\Big[\frac{\tilde\Omega}{\tilde\lambda_1}\,\tanh\frac{\tilde\lambda_1}{2T} + \frac{\tilde\Omega}{\tilde\lambda_2}\,\tanh\frac{\tilde\lambda_2}{2T}\Big],$$
$$\sigma^x = \frac{1}{2}\Big[\frac{\tilde\Omega}{\tilde\lambda_1}\,\tanh\frac{\tilde\lambda_1}{2T} - \frac{\tilde\Omega}{\tilde\lambda_2}\,\tanh\frac{\tilde\lambda_2}{2T}\Big];$$

values ξ^y, σ^y equal zero.

A free energy per model unit cell $f(4) = F(4)/(k_{\mathrm{B}}N)$ in the variables ξ^z and σ^z is the following:

$$f(4) = \frac{1}{2}\tilde v c_{44}^{E0}\varepsilon_4^2 - \tilde v e_{14}^0\varepsilon_4 E_1 - \frac{1}{2}\tilde v\chi_{11}^{\varepsilon 0}{E_1}^2 + \frac{1}{2}\Big[\tilde R_0^+(\xi^z)^2 + \tilde R_0^-(\sigma^z)^2\Big] - T\sum_f \ln\left(2\cosh\frac{\tilde\lambda_f}{2T}\right), \tag{17}$$

where $\tilde v = \dfrac{v}{k_{\mathrm{B}}}$. By differentiating free energy we can find dielectric, elastic, and piezoelectric properties of the Rochelle salt.

The conditions

$$\frac{1}{\tilde v}\left(\frac{\partial f(4)}{\partial\varepsilon_4}\right)_{E_1,T} = \sigma_4, \qquad \frac{1}{\tilde v}\left(\frac{\partial f(4)}{\partial E_1}\right)_{\varepsilon_4,T} = -P_1$$

yield the following expression for the stress σ_4 and polarization P_1:

$$\sigma_4 = c_{44}^{E0}\varepsilon_4 - e_{14}^0 E_1 + \frac{2\tilde\psi_4}{\tilde v}\xi^z, \tag{18a}$$

$$P_1 = e_{14}^0\varepsilon_4 + \chi_{11}^{\varepsilon 0}E_1 + \frac{\tilde\mu}{\tilde v}\xi^z. \tag{18b}$$

An independent variable is stress rather than deformation, so we need to express local fields in terms of σ_4 when solving system (14). Having used (18a) we derive

$$\varepsilon_4 = \frac{\sigma_4}{c_{44}^{E0}} + \frac{e_{14}^0}{c_{44}^{E0}}E_1 - \frac{2\tilde\psi_4}{\tilde v c_{44}^{E0}}\xi^z. \tag{19}$$

On the basis of Eq. (19) we can rewrite local fields in the following way:

$$\tilde\varepsilon_1 = \tilde R_0'^+\xi^z + \tilde R_0^-\sigma^z + \tilde\Delta - \frac{2\tilde\psi_4}{c_{44}^{E0}}\sigma_4 + \tilde\mu' E_1, \tag{20a}$$

$$\tilde\varepsilon_2 = \tilde R_0'^+\xi^z - \tilde R_0^-\sigma^z - \tilde\Delta - \frac{2\tilde\psi_4}{c_{44}^{E0}}\sigma_4 + \tilde\mu' E_1, \tag{20b}$$

where $\tilde R'^+$ and $\tilde\mu'$ are the following:

$$\tilde R_0'^+ = \tilde R_0^+ + \frac{4{\tilde\psi_4}^2}{\tilde v c_{44}^{E0}}, \quad \tilde\mu' = \tilde\mu - \frac{2\tilde\psi_4 e_{14}^0}{c_{44}^{E0}}. \tag{21}$$

System (14) with local fields (20), considered at $\sigma_4 = 0$, $E_1 = 0$, has solutions of two types: $\xi^z = 0$ and $\xi^z \neq 0$. The minimum free energy (17) condition defines which of the solutions is actually realized at each particular T. The solution of the first type describes a paraelectric phase and the solution of the second type describes a ferroelectric phase. In a paraelectric phase we have also $\sigma^x = 0$.

We calculate longitudinal dielectric susceptibility of the clamped crystal by differentiating Eq. (18b):

$$\chi_{11}^{\varepsilon} = \left(\frac{\partial P_1}{\partial E_1}\right)_{\varepsilon_4} = \chi_{11}^{\varepsilon 0} + \frac{\tilde{\mu}}{\tilde{v}}\left(\frac{\partial \xi^z}{\partial E_1}\right)_{\varepsilon_4}. \qquad (22)$$

Hereinafter the derivatives are taken at constant T.

We derive the value $\left(\frac{\partial \xi^z}{\partial E_1}\right)_{\varepsilon_4}$ by differentiating Eq. (14). After making the necessary transformations:

$$\chi_{11}^{\varepsilon} = \chi_{11}^{\varepsilon 0} + \frac{\tilde{\mu}^2}{\tilde{v}} f_1(\xi^z, \sigma^z), \qquad (23)$$

where

$$f_1(\xi^z, \sigma^z) = \frac{e_1 - \tilde{R}_0^-({e_1}^2 - {e_2}^2)}{1 - e_1(\tilde{R}_0^+ + \tilde{R}_0^-) + \tilde{R}_0^+\tilde{R}_0^-({e_1}^2 - {e_2}^2)} \qquad (24)$$

and the following notations are used:

$$\begin{aligned} e_1 &= \frac{a_1 + a_2}{4T} + \frac{\tilde{\Omega}^2(b_1 + b_2)}{2}, \\ e_2 &= \frac{a_1 - a_2}{4T} + \frac{\tilde{\Omega}^2(b_1 - b_2)}{2}, \\ a_i &= \frac{\tilde{\varepsilon}_i^2}{\tilde{\lambda}_i^2} - {\eta_i}^2, \quad b_i = \frac{\eta_i}{\tilde{\varepsilon}_i\tilde{\lambda}_i^2}, \qquad i = 1, 2; \\ \eta_1 &= \xi^z + \sigma^z, \quad \eta_2 = \xi^z - \sigma^z. \end{aligned} \qquad (25)$$

The static dielectric susceptibility of free crystal

$$\chi_{11}^{\sigma} = \left(\frac{\partial P_1}{\partial E_1}\right)_{\sigma_4} = \chi_{11}^{\sigma 0} + \frac{\tilde{\mu}'}{\tilde{v}}\left(\frac{\partial \xi^z}{\partial E_1}\right)_{\sigma_4}$$

is as follows

$$\chi_{11}^{\sigma} = \chi_{11}^{\sigma 0} + \frac{\tilde{\mu}'^2}{\tilde{v}} f_2(\xi^z, \sigma^z), \qquad (26)$$

where

$$\chi_{11}^{\sigma 0} = \chi_{11}^{\varepsilon 0} + \frac{(e_{14}^0)^2}{c_{44}^{E0}}, \qquad (27)$$

where a function $f_2(\xi^z, \sigma^z)$ is used

$$f_2(\xi^z, \sigma^z) = \frac{e_1 - \tilde{R}_0^-({e_1}^2 - {e_2}^2)}{1 - e_1(\tilde{R}_0'^+ + \tilde{R}_0^-) + \tilde{R}_0'^+\tilde{R}_0^-({e_1}^2 - {e_2}^2)}, \qquad (28)$$

and $\tilde{\mu}'$, $\tilde{R}_0'^+$ are presented in (21).

The coefficient of the piezoelectric stress is the following:

$$e_{14} = \left(\frac{\partial P_1}{\partial \varepsilon_4}\right)_{E_1} = e_{14}^0 - \frac{2\tilde{\mu}\tilde{\psi}_4}{\tilde{v}} f_1(\xi^z, \sigma^z). \qquad (29)$$

The elastic constant at a constant field:

$$c_{44}^{E} = \left(\frac{\partial \sigma_4}{\partial \varepsilon_4}\right)_{E_1} = c_{44}^{E0} - \frac{4\tilde{\psi}_4^2}{\tilde{v}} f_1(\xi^z, \sigma^z). \qquad (30)$$

The coefficient of the piezoelectric strain:

$$d_{14} = \left(\frac{\partial P_1}{\partial \sigma_4}\right)_{E_1} = d_{14}^0 - \frac{2\tilde{\mu}'\tilde{\psi}_4}{\tilde{v}c_{44}^{E0}} f_2(\xi^z, \sigma^z), \qquad (31)$$

where

$$d_{14}^0 = \frac{e_{14}^0}{c_{44}^{E0}}. \qquad (32)$$

The values χ_{11}^{σ}, d_{14} could be alternatively derived through e_{14}, c_{44}^{E} and χ_{11}^{ε}:

$$\chi_{11}^{\sigma} = \chi_{11}^{\varepsilon} + \frac{(e_{14})^2}{c_{44}^{E}}, \quad d_{14} = \frac{e_{14}}{c_{44}^{E}}.$$

We derive molar entropy of the pseudospin subsystem of the considered model in the form:

$$\begin{aligned} S &= -\frac{R}{2}\left(\frac{\partial f(4)}{\partial T}\right)_{E_1,\varepsilon_4} \\ &= \frac{R}{2}\left\{\sum_f \left[\ln\left(2\cosh\frac{\tilde{\lambda}_f}{2T}\right) - \frac{\tilde{\lambda}_f}{2T}\tanh\frac{\tilde{\lambda}_f}{2T}\right]\right\}, \end{aligned} \qquad (33)$$

where R is gas constant.

We calculate the molar specific heat of the pseudospin subsystem at constant stress and the electric field by a numerical differentiation of the entropy:

$$\Delta C^{\sigma E} = T\left(\frac{\partial S}{\partial T}\right)_{\sigma_4, E_1}. \qquad (34)$$

In the present work the calculation of thermodynamic characteristics is carried out at $\sigma_4 = 0$, $E_1 = 0$.

We may notice that at $\tilde{\Omega} = 0$ all the results of the present work coincide with those of the previous calculations [20] where transverse field was not taken into account. If we neglect piezoelectric interaction, our results will coincide with the other results [13] where the Mitsui model with a transverse field and without piezoelectric interaction was considered.

III. DISCUSSION

A. Theory model parameters selection procedure

The proposed model was used for the analysis of physical properties of the Rochelle salt crystal that is not externally affected ($E_1 = 0$, $\sigma_4 = 0$). To obtain specific numerical results it is necessary first of all to identify theory model parameters for calculations. The following parameters should be identified:

$$\tilde{\Omega}, \quad \tilde{J}_0, \quad \tilde{K}_0, \quad \tilde{\Delta}, \quad \tilde{\psi}_4, \quad \tilde{\mu}, \quad c_{44}^{E0}, \quad e_{14}^0, \quad \chi_{11}^{\varepsilon 0},$$

in which case the parameter $\tilde{\mu}$ will be considered as linearly dependent on temperature. These parameters should provide the best agreement between the theory and experiment jointly for thermodynamic and dynamic characteristics. We will describe the procedure for parameters selection only in general terms.

First of all, theory model parameters must provide two second order phase transitions as is exhibited by experiment. The problem of the Mitsui model phase behavior dependence on theory parameters in molecular field approximation was solved [29], and the complete phase diagram of the Mitsui model in the presence of a transverse field was constructed. However, piezoelectric interaction was not considered. We shall use these results for selecting theory parameters.

It is convenient to present phase diagram of the Mitsui model in terms of relative parameters ω, γ, a, t. In our case for the model with piezoelectric interaction relative parameters are expressed through theory model parameters in the following way:[3]

$$\omega = \frac{\tilde{\Omega}}{2\tilde{R}_0'^{+}}, \quad \gamma = \frac{\Delta}{2\tilde{R}_0'^{+}}, \quad a = -\frac{\tilde{R}_0^{-}}{\tilde{R}_0'^{+}}, \quad t = \frac{T}{2\tilde{R}_0'^{+}}.$$

So, phase behavior of the model is completely determined by relative parameters ω, γ, a. Herewith, for any set of these parameters, which provide two second order phase transitions, it is always possible to find such parameter $\tilde{R}_0'^{+}$ and respectively $\tilde{\Omega}$, $\tilde{R}_0^{-}$, $\tilde{\Delta}$, which will make it possible to derive a correct (experimental) temperature of lower phase transition. Basing on this condition with certain ω, γ, a we derived parameters $\tilde{R}_0'^{+}$, $\tilde{\Omega}$, $\tilde{R}_0^{-}$, $\tilde{\Delta}$.

Figure 1 illustrates phase diagram of the Mitsui model without transverse field, and Fig. 2 illustrates phase diagram of the Mitsui model with transverse field $\omega = 0.10$. In both cases, the figures illustrate a complete phase diagram and a certain region thereof in an expanded view. Each of the microparameters regions on the phase diagrams corresponds to a certain sequence of phase transitions, which occur as the temperature rises.

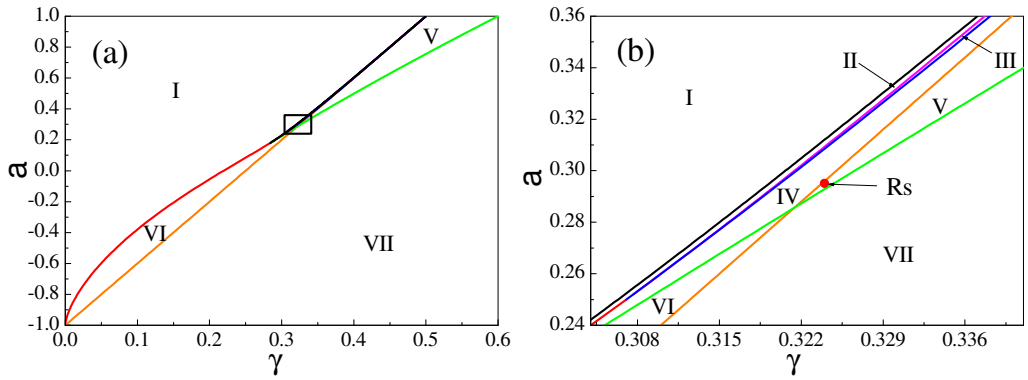

Fig. 1. Phase diagram of the Mitsui model without transverse field. Complete phase diagram is presented (a) where the rectangle denotes the region shown in expanded view (b). A point corresponds to the parameters for Rochelle salt derived earlier [20].

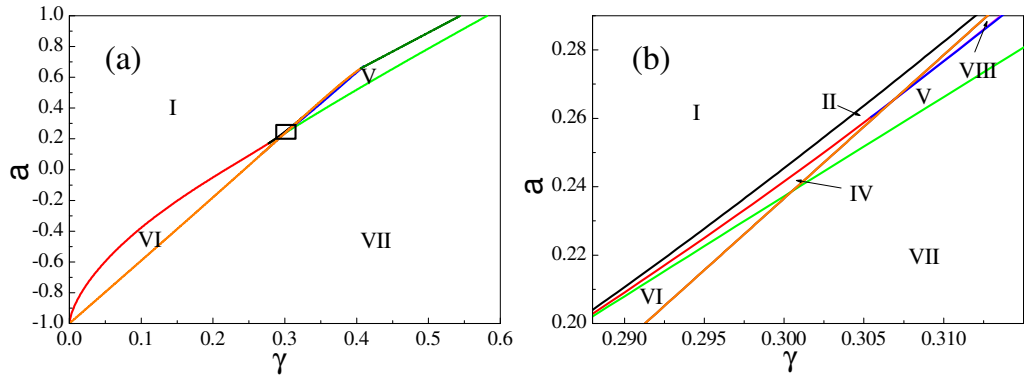

Fig. 2. Phase diagram of the Mitsui model with a transverse field $\omega = 0.10$. Complete phase diagram is presented (a) where the rectangle denotes the region shown in the expanded view (b).

[3]Accounting for piezoelectric interaction in phase diagram results in the change of parameter $\tilde{R}_0^{+}$ into $\tilde{R}_0'^{+}$. This can be seen when we analyze Eq. (14) and expressions for local fields in the form of (20) both for the model with piezoelectric interaction and the one without it.

Herein below we specify what particular phase transitions occur in each of these regions.

I — ground state is ordered; 2nd order p.t. (phase transitions) from ordered into disordered state;

II — ground state is ordered; two low temperature 1st order p.t. and one 2nd order p.t.;

III — ground state is ordered; 1st order p.t.(from ordered into disordered state), 2nd order p.t. (from disordered into ordered state), 1st order p.t. within ferroelectric phase and 2nd order p.t. into disordered state;

IV — ground state is ordered; one low temperature 1st order p.t. and two 2nd order p.t.;

V — ground state is disordered; two 2nd order p.t. (Rs *crystal case*)

VI — ground state is disordered; one 1st order p.t.;

VII — no phase transitions, disordered state is steady;

VIII — ground state is disordered; one low temperature 1st order p.t. and one 2nd order p.t.

Apart from the regions specified above, there are other regions which due to their small sizes are virtually unnoticeable on the phase diagram. Herein below we also specify the sequences of phase transitions in these regions.

IX — ground state is disordered; low temperature 2nd order p.t., 1st order p.t. within ferroelectric phase and one 2nd order p.t.;

X — ground state is ordered; one 1st order p.t. within ferroelectric phase and one 2nd order p.t.

XI — ground state is ordered; two low temperature 1st order p.t., and 2nd order p.t.;

XII — ground state is disordered; two low temperature 1st order p.t., 2nd order p.t., 1st order p.t. within ferroelectric phase and one 2nd order p.t.;

XIII — ground state is disordered; two low temperature 1st order p.t., one 2nd order p.t.;

XIV — ground state is disordered; two 1st order p.t.

Regions I–VII are shown on the phase diagrams of models with a transverse field and on the diagrams of models without a transverse field; regions VIII — XIV are observed only on the phase diagram of the model with a transverse field. As is seen from the phase diagrams, the parameters for the Rochelle salt crystal should be selected from region V.

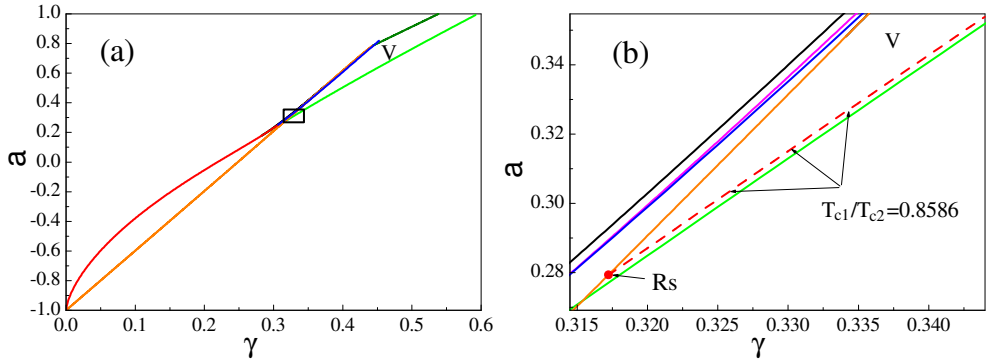

Fig. 3. Phase diagram of the Mitsui model with transverse field $\omega = 0.05$. Complete phase diagram is presented (a) where rectangle denotes the region shown in expanded view (b). Dashed line corresponds to the low and upper phase transitions temperature value ratio observed for Rs. A point corresponds to the parameters, which describe physical properties of Rs crystal in the best way.

Figure 3 presents the phase diagram of the Mitsui model with a transverse field $\omega = 0.05$, and particularly a region with two second order phase transitions. Also this figure shows a line, which corresponds to the experimental phase transitions temperatures value the ratio for Rs crystal: $T_{c1}/T_{c2} = 0.8586$ ($T_{c1} = 255$ K, $T_{c2} = 297$ K). A point on the phase diagram, which corresponds to the parameters γ and a, describes physical properties of Rochelle salt, it must be located on the specified line. Thus, there is only one degree of freedom for the selection of the pair γ, a. As was mentioned above, for each point of this line one can define such a value of parameter $\tilde{R}_0'^{+}$, which will ensure the proper temperature value of a low phase transition; together with the temperature of a low phase transition the temperature of the upper phase transition will correspond to the experimental value.

At set ω, γ, $\tilde{\psi}_4$ (parameter a at the known γ was determined granting that $T_{c1}/T_{c2} = 0.8586$) and calculated $\tilde{R}_0'^{+}$ we derived the parameters c_{44}^{E0}, e_{14}^{0}, $\chi_{11}^{\varepsilon 0}$, $\mu(T)$ basing on the following conditions:

1) theoretically calculated elastic constant agrees with the experimental one at the temperature point located approximately in the middle of the ferroelectric phase: $T = 274.12$ K, $c_{44}^{E} = 7.7873 \times 10^{-11}$ N/m^2 [30], basing on this condition parameter c_{44}^{E0} was determined;

2) theoretically calculated dielectric susceptibility of a clamped crystal agrees with the experimental one at the points of phase transitions: $\chi_{11}^{\varepsilon}(T_{c1}) = 1/0.045$, $\chi_{11}^{\varepsilon}(T_{c2}) = 1/0.054$ [5], basing on this condition (with the already known c_{44}^{E0}) the effective dipole moment $\mu(T)$ was determined;

3) theoretically calculated dielectric susceptibility of a clamped crystal agrees with the experimental one in a high temperature paraelectric phase: $T_m = 313$ K, $\chi_{11}^{\varepsilon}(T_m) = 1/0.151$ [5];

4) theoretically calculated dielectric susceptibility of a free crystal agrees with the experimental one in a high temperature paraelectric phase: $T_l = 312.71$ K, $\chi_{11}^{\sigma}(T_l) = 1/0.0912$ [31]. Basing on this and previous

condition (with the known c_{44}^{E0} and $\mu(T)$) parameters e_{14}^{0} and $\chi_{11}^{\varepsilon 0}$ were jointly determined.

We shall consider the volume of a model unit cell to equal [32]:

$$v = 5.219 \times 10^{-22} \text{ cm}^3.$$

Thus, at each fixed transverse field two values remain unknown: the point of parameters (γ, a) on a phase diagram line (Fig. 3 b) and parameter $\tilde{\psi}_4$. Having different transverse fields we searched for these two unknown values on the basis of the best agreement between theory and experiment for thermodynamic characteristics: P_1, ε_4, $1/\chi_{11}^{\varepsilon}$, $1/\chi_{11}^{\sigma}$, e_{14}, d_{14}, c_{44}^{E}. As a result we derived that the best agreement is achieved when the point of parameters (γ, a) is located on the border of region V, for instance, as is illustrated in Fig. 3. At all the values of a transverse field for border point of parameters (γ, a) there is an optimal value of parameter $\tilde{\psi}_4$, which provides the best description of physical properties.

Such parameters selection procedure was applied to the model with several different values of transverse fields and it was derived that at each transverse field the specified procedure leads to equally good agreement between theory and experiment for all thermodynamic characteristics except for polarization. At zero-value transverse field theoretically calculated saturation polarization is considerably lower than its experimental value. With the rise of a transverse field, saturation polarization rises too. With the transverse field $\omega = 0.05$ (for a border point on a phase diagram $\gamma = 0.3172$, $a = 0.2794$; $\tilde{R}_0'^{+} = 1134.67$ K) theoretically calculated saturation polarization comes up to its experimental value. Derived by this means a transverse field is considered to be optimal for the description of physical properties of the Rochelle salt crystal and thus, we believe that the issue of theory parameters selection is solved.

	$\omega = 0.0$	$\omega = 0.05$
$\tilde{\Omega}$ (K)	0.0	113.467
$\tilde{J}_0$ (K)	797.36	813.216
$\tilde{K}_0$ (K)	1468.83	1447.17
$\tilde{\Delta}$ (K)	737.33	719.937
$\tilde{\psi}_4$ (K)	−760.0	−720.0
c_{44}^{E0} (10^{10} N/m^2)	1.28	1.224
e_{14}^{0} (10^{-2} C/m^2)	3.336	31.64
$\chi_{11}^{\varepsilon 0}$	0.318	0.0
$\mu(T) = a + k(T - 297)$		
a (10^{-30} Cm)	8.41	8.157
k (10^{-30} Cm/K)	−0.022	−0.0185

Table 1. Optimal values of theory parameters for Rochelle salt. Two parameters sets for the models with and without transverse field are presented.

Table 1 presents theory parameters, which we derived within the model with a transverse field, along with the parameters, derived within the analogous model without transverse field. Generally, in comparison with the model without transverse field, the parameters varied only slightly. The only exception is the parameter e_{14}^{0}, which increased almost tenfold. This is connected, most likely, with a somewhat different procedure for the theory parameters selection which was applied for the model without a transverse field.

B. Dielectric, elastic and piezoelectric properties

The results of calculations made for static dielectric characteristics on the basis of a model with and without transverse field (with the corresponding theory parameters, presented in Table 1) are shown in Fig. 4 together with experimental data.

The derived dependency of polarization on temperature in case with the model with a transverse field agrees with experimental data significantly better than in the case with the model without transverse field. Specifically, we managed to achieve experimental value of saturation polarization within the model with transverse field. It must be noted that we managed to achieve the rise of saturation polarization not due to the rise of effective dipole moment as far as accounting for transverse field resulted in the reduction of effective dipole moment. So, the rise of saturation polarization can be considered to be caused by the accounting for transverse field. However, contrary to experiment, theoretically calculated polarization is substantially asymmetrical (temperature of saturation polarization is significantly shifted towards low phase transition), and accounting for a transverse field failed to correct this discrepancy.

Accounting for a transverse field improved the agreement between theory and experiment as regards spontaneous deformation to a certain extent.

Dielectric permittivity of a clamped crystal, calculated within the model with transverse field, has a better agreement with experiment than the one calculated without a transverse field. Also we managed to improve the agreement between theory and experiment in ferroelectric phase and in low temperature phase for this characteristics. What concerns a free crystal permittivity and elastic constant c_{44}^{E}, accounting for transverse field did not result in any noticeable changes. In the same manner as for the model without a transverse field, there was no agreement between theory and experiment reached for both of these characteristics in the low temperature phase. What concerns the coefficients of piezoelectric stress and deformation e_{14}, d_{14}, accounting for a transverse field provided better agreement between theory and experiment in the ferroelectric phase, and in a high temperature paraelectric phase agreement between theory and experiment remained almost unchanged.

Accounting for transverse field to some extent increased molecular specific heat value. However, in general its temperature behavior remained unchanged. Considering that presently there are no reliable experimental data for specific heat we left the issue of agreement between theory and experiment for this characteristics unconsidered. The issue of inconsistency between the measurements for specific heat presented by different experimental works was discussed [20].

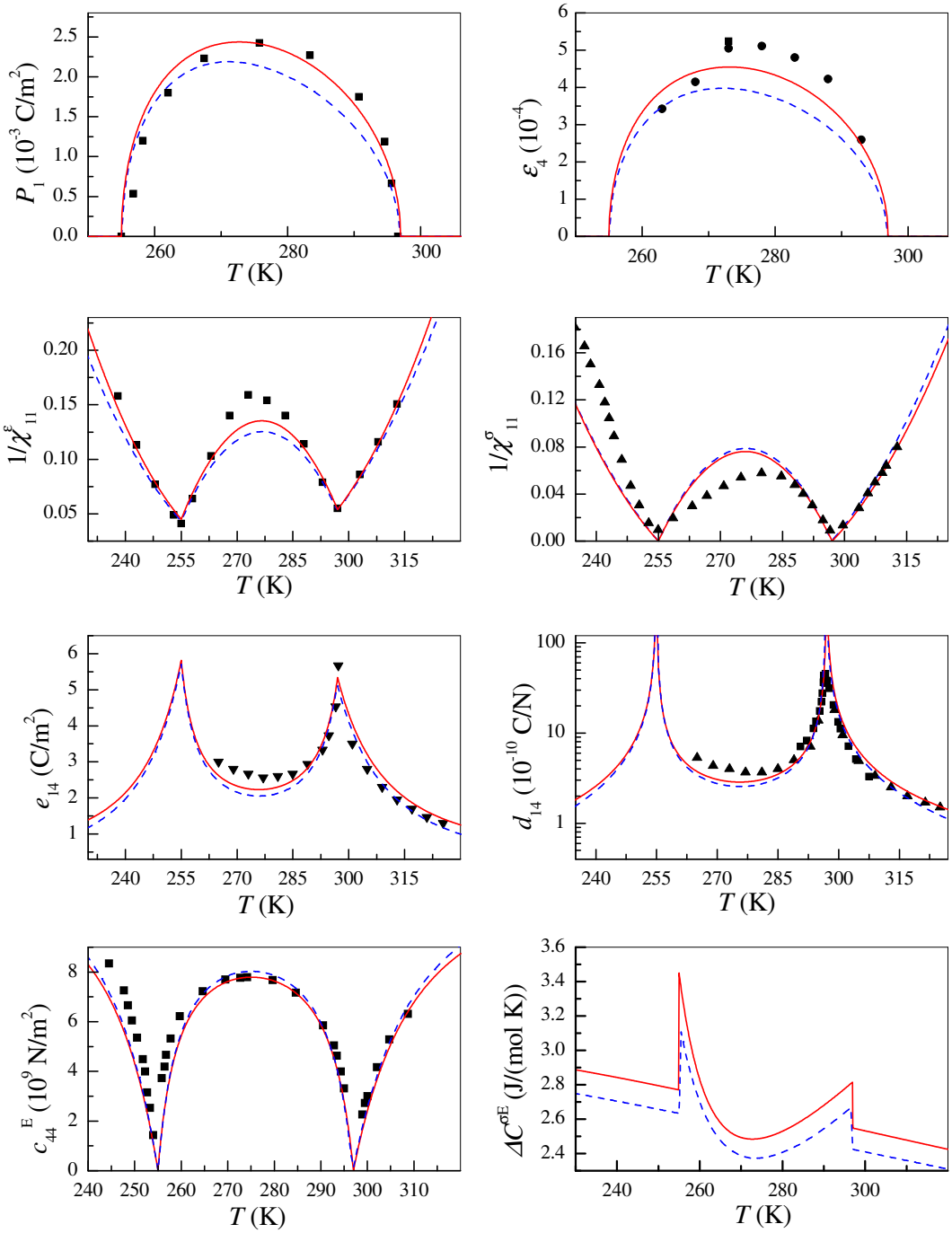

Fig. 4. Theoretical and experimental physical characteristics of the Rochelle salt. Solid line corresponds to calculations, carried out at $\omega = 0.05$, dashed line corresponds to calculations, carried out at $\omega = 0.00$. Points are the experimental data. $P_1(T)$: ■ (Ref. [33]), $\varepsilon_4(T)$: ■ (Ref. [34]), • ($P_1 d_{14}/\chi^{\sigma}_{11}$: Ref. [33]), $1/\chi^{\varepsilon}_{11}(T)$: ■ (Ref. [5]), $1/\chi^{\sigma}_{11}(T)$: ▲ (Ref. [31]), $e_{14}(T)$: ▼ (Ref. [35]), $d_{14}(T)$: ■ (Ref. [35]), ▲ (Ref. [36]), c^{E}_{44}: ■ (Ref. [30]).

With regard to the results obtained for spontaneous polarization and dielectric permittivity of a free crystal, one remark should be made. The level of agreement between theory and experiment for spontaneous polarization and dielectric permittivity of a free crystal can be regulated by dipole moment altering. Thus, if we assume that a true dependence of a dipole moment on temperature is weaker, specifically if we assume that at the lower phase transition point a dipole moment is a little smaller and at the upper phase transition point a dipole moment is a little higher, we can expect that it will be possible to eliminate asymmetry of polarization and at the same time to agree theoretically calculated dielectric permittivity of a free crystal with experiment in a low temperature paraelectric phase. It should be noticed that alteration of effective dipole moment will have no effect on calculated elastic constant and respectively is not able to improve agreement between theory and experiment in low temperature paraelectric phase for this characteristics.

IV. CONCLUSIONS

In this work we supplemented the Mitsui model extended by piezoelectric interaction with a transverse field. By accounting for a transverse field, we successfully attempted to resolve the current problem of erroneously low theoretically calculated polarization as compared to the experimental data.

Within the framework of the conducted research we managed to select the set of parameters, which ensured the close agreement between theory and experiment for dielectric, elastic and piezoelectric properties of the Rochelle salt. Comparing the earlier derived results for the model without transverse field with the results derived in this work, one may state that it is the consideration of transverse field that is the necessary condition for achieving agreement between theory and experiment for polarization. Thereby the effective dipole moment derived within the model with a transverse field is even lower than within the model without a transverse field. The outstanding issues still include poor agreement between theory and experiment for the elastic constant c_{44}^E and static dielectric permittivity of free crystal χ_{11}^σ in a low-temperature paraelectric phase. Besides, theoretically calculated temperature dependence of polarization is of asymmetrical shape with the temperature of polarization saturation shifted towards lower phase transition, while the experiment demonstrated the symmetrical shape of temperature dependence of polarization.

We noticed that the insufficient agreement between theory and experiment for spontaneous polarization (its asymmetry), static dielectric permittivity of free crystal and high-frequency permittivity in a low-temperature paraelectric phase can be remedied by a slight adjustment of the dipole moment dependence on temperature. Specifically, if we assume that the dipole moment dependence on temperature is weaker than that obtained by us, it is possible to achieve a significantly better agreement between theory and experiment for the properties stated above.

Using additional term (transverse field) in Hamiltonian allows us to expect a more correct dynamic behavior of the system. So, we expect to derive two types of dynamics for the Rochelle salt within the extended model: relaxation dynamics (microwave region) and resonance dynamics as observable in the experiment. We will study this issue further.

ACKNOWLEDGEMENT

The authors are grateful to Professor Ihor Stasyuk for his kind interest in the work and particularly for discussing the nature of a transverse field in the Hamiltonian.

[1] F. Jona, G. Shirane, *Ferroelectric crystals* (Pergamon Press Inc., Oxford, 1962).
[2] X. Solans, C. Gonzalez-Silgo, C. Ruiz-Pérez, J. Solid State Chem. **131**, 350 (1997).
[3] J. Kulda, J. Hlinka, S. Kamba, J. Petzelt, ILL: Annual Report 2000.
[4] H. E. Müser, J. Pottharst, Phys. Status Solidi **24**, 109 (1967).
[5] F. Sandy, R. V. Jones, Phys. Rev. **168**, 481 (1968).
[6] H. Kolodziej, in: *Dielectric and Related Molecular Processes, Vol. 2* (The Chemical Society Burlington House, London, 1975), p. 249.
[7] Y. Iwata, S. Mitani, O. Shibuya, Ferroelectrics **107**, 287 (1990).
[8] A. A. Volkov, Yu. G. Goncharov, G. V. Kozlov, Ye. B. Kryukova, J. Petzelt, Pis'ma Zh. Éksp. Teor. Fiz. **41**, 16 (1985). [JETP Lett. **41**, 17 (1985)].
[9] S. Kamba, G. Schaack, J. Petzelt, Phys. Rev. B **51**, 14998 (1995).
[10] J. Hlinka, J. Kulda, S. Kamba, J. Petzelt, Phys. Rev. B **63**, 052102 (2001).
[11] T. Mitsui, Phys. Rev. **111**, 1259 (1958).
[12] B. Žekš , G. G. Shukla, R. Blinc, Phys. Rev. B **3**, 2306 (1971).
[13] V. G. Vaks, *Introduction into Microscopic Theory of Ferroelectrics* (Nauka, Moscow, 1973) (in Russian).
[14] J. Kalenik, Acta Phys. Pol. **A48**, 387 (1975).
[15] K. Mori, Ferroelectrics **31**, 173 (1981).
[16] B. Žekš, G. G. Shukla, R. Blinc, J. Phys. Colloq., Suppl. **33**, C2 (1972).
[17] R. R. Levitskii, I. R. Zachek, V. I. Varanitskii, Ukr. Phys. J. **25**, 1766 (1980) (in Russian).
[18] R. R. Levitskii, I. R. Zachek, V. I. Varanitskii, Fiz. Tverd. Tela (Leningrad) **22**, 2750 (1980) [Sov. Phys. Solid State **22**, 1603 (1980)].
[19] R. R. Levitskii, Yu. T. Antonyak, I. R. Zachek, Ukr. Phys. J. **26**, 1835 (1981) (in Russian).
[20] R. R. Levitskii, I. R. Zachek, T. M. Verkholyak, A. P. Moina, Phys. Rev. B **67**, 174112 (2003).
[21] A. P. Moina, A. G. Slivka, V. M. Kedyulich, Phys. Status Solidi B. **244**, 2641 (2007).
[22] R. R. Levitskii, A. P. Moina, A. Ya. Andrusyk, A. G. Slivka, V. M. Kedyulich, J. Phys. Stud. **11**, 2603 (2008).
[23] R. R. Levitskii, I. R. Zachek, A. P. Moina, T. M. Verkholyak, J. Phys. Stud. **7**, 106 (2003).
[24] R. R. Levitskii, I. R. Zachek, A. P. Moina, A. Ya. Andrusyk, Condens. Matter Phys. **7**, 111 (2004).
[25] A. P. Moina, R. R. Levitskii, I. R. Zachek, Phys. Rev. B **71**, 134108 (2005).
[26] A. G. Slivka, V. M. Kedyulich, R. R. Levitskii, A. P. Moina, M. O. Romanyuk, A. M. Guivan, Condens. Matter Phys. **8**, 623 (2005).
[27] I. V. Stasyuk, O. V. Velychko, Ferroelectrics **316**, 51 (2005).
[28] R. R. Levitskii, T. M. Verkholyak, I. V. Kutny, I. G. Hil', cond-mat/0106351 (unpublished).
[29] Yu. I. Dublenych, preprint/ICMP-02-15U (unpublished).

[30] O. Yu. Serdobolskaya, Solid State Phys. **38**, 1529 (1996).
[31] W. Taylor, D. J. Lockwood, H. J. Labbe, J. Phys. C.: Solid State Phys. **17**, 3685 (1984).
[32] W. J. Bronowska, J. Appl. Crystallogr. **14**, 203 (1981).
[33] W. G. Cady, *Piezoelectricity; An Introduction to the Theory and Application of Electromechanical Phenomena in Crystals* (McGraw Hill, New York, 1946).
[34] A. R. Ubbelohde, I. Woodward, Proc. R. Soc. **185**, 448 (1946).
[35] L. Gutin, Zh. Éksp. Teor. Fiz. **15**, 199 (1945).
[36] H. Beige, A. Kühnel, Phys. Status Solidi A **84**, 433 (1984).

ВИВЧЕННЯ ТЕРМОДИНАМІЧНИХ ВЛАСТИВОСТЕЙ КРИСТАЛУ СЕГНЕТОВОЇ СОЛІ $NaKC_4H_4O_6{\cdot}4H_2O$ В МЕЖАХ МОДЕЛІ МІЦУЇ З УРАХУВАННЯМ П'ЄЗОЕЛЕКТРИЧНОЇ ВЗАЄМОДІЇ ТА ПОПЕРЕЧНОГО ПОЛЯ

Р. Р. Левицький[1], І. Р. Зачек[2], А. Я. Андрусик[1]
[1] *Інститут фізики конденсованих систем НАН України, вул. Свенціцького, 1, Львів, 79011, Україна*
[2] *Національний Університет "Львівська політехніка", кафедра загальної фізики, вул. С. Бандери, 12, Львів, 79013, Україна*

У межах моделі Міцуї, що враховує п'єзоелектричну взаємодію та поперечне поле, розраховано діелектричні, п'єзоелектричні та пружні характеристики сеґнетової солі. Наявність поперечного поля пов'язано з можливістю динамічних перескоків структурних елементів між двома положеннями рівноваги. Розрахунки проводили в наближенні молекулярного поля. Показано, що за відсутності поперечного поля чи п'єзоелектричної взаємодії отримані результати збігаються з одержаними раніше.

Для отримання конкретних числових результатів запропоновано процедуру вибору модельних параметрів теорії, яка використовує фазову діаграму моделі Міцуї. Показано, що врахування п'єзоелектричної взаємодії не змінює самої фазової діаграми, а лише перенормовує параметри теорії, у яких вона будується. У статті наведено повну фазову діаграму моделі Міцуї (як із поперечним полем, так і без нього) а також указано, яку послідовність фазових переходів зазнає система, параметри якої відповідають кожній з областей діаграми.

Запропонована процедура дала змогу одержати оптимальний набір параметрів теорії, який сукупно для термодинамічних характеристик забезпечив найкраще узгодження теорії з експериментом. У цій статті показано, що врахування поперечного поля дає змогу досягнути кращого узгодження теорії з експериментом для термодинамічних характеристик порівняно з аналогічними результатами, отриманими в межах моделі без поперечного поля. Зокрема саме врахуванням поперечного поля було досягнуто прийнятного узгодження теорії з експериментом для спонтанної поляризації.